ELSEVIER

Journal of Neuroscience Methods 152 (2006) 173–178

JOURNAL OF NEUROSCIENCE METHODS

www.elsevier.com/locate/jneumeth

Respiratory cycle as time basis: An improved method for averaging olfactory neural events

Stéphane G. Roux [a], Samuel Garcia [b], Bernard Bertrand [b], Tristan Cenier [b], Michel Vigouroux [b], Nathalie Buonviso [b], Philippe Litaudon [b,*]

[a] *Laboratoire de Physique, Ecole Normale Supérieure de Lyon, 46 allée d'Italie, 69364 Lyon cedex 07, France*
[b] *Neurosciences et Systèmes Sensoriels, Université Lyon I-CNRS, 50 Avenue Tony Garnier, 69366 Lyon cedex 07, France*

Received 20 May 2005; received in revised form 2 September 2005; accepted 2 September 2005

Abstract

In the mammalian olfactory system, neural activity appears largely modulated by respiration. Accurate analysis of respiratory synchronized activity is precluded by the variability of the respiratory frequency from trial to trial. Thus, the use of respiratory cycle as the time basis for measuring cell responses was developed about 20 years ago. Nevertheless, averaging oscillatory component of the activity remains a challenge due to their rhythmic features. In this paper, we present a new respiratory monitoring setup based on the measurement of micropressure changes induced by nasal airflow in front of the nostril. Improvements provided by this new monitoring setup allows automatic processing of respiratory signals in order to extract each respiratory period (expiration and inspiration). The time component of these periods, which can differ from trial to trial, is converted into a phase component defined as $[-\pi, 0]$ and $[0, \pi]$ for inspiration and expiration, respectively. As opposed to time representation, the phase representation is common to all trials. Thus, this phase representation of the respiratory cycle is used as a normalized time basis permitting to collect results in a standardized data format across different animals and providing new tools to average oscillatory components of the activity.

Keywords: Rat; Olfaction; Respiratory monitoring; Time–frequency analysis; Data averaging

1. Introduction

In terrestrial vertebrates, olfactory perception depends on respiration. Olfactory receptors are situated in the nasal cavity and odor molecules must be transported by the inhaled air to evoke a response. As far back as the very first electrophysiological works, the powerful influence of breathing was noticed in the olfactory bulb (OB) and olfactory cortex (OC). Already Adrian (1950) had pointed out that the velocity of the air through the nose was the principal factor in determining what he called "induced waves" in OB and cortex. He observed that such a rhythmical activity appeared at each inspiration. Respiratory modulation of electro-encephalographic (EEG) and local field potential (LFP) signals has been extensively described in OB and OC (Boudreau and Freeman, 1963; Buonviso et al., 2003; Fontanini et al., 2003; Freeman, 1975, 1983; Freeman and Schneider, 1982). Such a respiratory modulation has also been described in cell unitary activities in the OB mitral/tufted (Chaput, 1986; Chaput and Holley, 1980; Macrides and Chorover, 1972; Mair, 1982; Onoda and Mori, 1980; Pager, 1985; Walsh, 1956) and was recently described in the piriform cortex (PC) (Litaudon et al., 2003; Wilson, 1998). Rather than a variation in overall firing frequency, odor-evoked cell responses have often been reported as a temporal reorganization of their discharges into inhalation-related bursts of spikes. Respiratory cycle-triggered raster plots were used to classify response patterns as a function of the respiratory activity (Buonviso et al., 1992, 2003; Chaput et al., 1992; Litaudon et al., 2003; Wilson, 1998) and the inhalation/exhalation transition period appeared as a crucial time-window for both OB and cortical activity. All these data emphasize the rhythmic features of both LFP oscillatory activity and cell unitary discharges and their variability in the course of the respiratory cycle. A representation of the average unitary activity during the whole respiratory cycle does not take into account these features. Conversely, an accurate evaluation of the cell response requires a separate processing of the inspiration and expiration-related activity (Chaput and Holley, 1980). Recent data support the hypothesis that the respiratory

* Corresponding author. Tel.: +33 4 37 28 74 61; fax: +33 4 37 28 76 01.
E-mail address: litaudon@olfac.univ-lyon1.fr (P. Litaudon).

0165-0270/$ – see front matter © 2005 Elsevier B.V. All rights reserved.
doi:10.1016/j.jneumeth.2005.09.004

modulation itself could carry some information about the odor. Indeed, odorant stimulation has been shown to induce a respiration synchronized activation at the glomerular level whose amplitude, phase and spatial distribution are modulated in an odor-specific manner (Spors and Grinvald, 2002). Thus, odor identity and concentration are represented by spatio-temporal patterns, and the respiratory cycle might serve a role in reformatting spatially organized olfactory inputs (Margrie and Schaefer, 2003).

Thus, it appears necessary to take into account the time course of the respiratory cycle in different phases in order to analyze and average olfactory neural events. Such analysis needs accurate breathing recordings which can be carried out through different methods: airflow measurement (Johnson et al., 2003), temperature fluctuations (Chaput and Holley, 1980; Macrides et al., 1982) and piezoelectric monitoring of respiration associated chestwall movement (Wilson, 1998). The choice of a method depends on the respiratory variable that has to be evaluated (airflow, volume, time course, frequency, ...). Since our aim is to study precise temporal relationship between neural activity and respiratory activity in anesthetized animal, we focus on analyzing accurately the respiratory cycle time course with a particular concern to the detection of period changes. Therefore, respiratory sensors must present several compulsory features. First, the bandwidth must be adapted to the respiratory fluctuation frequency; second, hysteresis must be limited to avoid jitter; third, response latency must be as low as possible for the phase shift to be as small as possible. In this paper, we describe a respiratory monitoring setup based on a bidirectional airflow sensor. This setup allows accurate recording of inhalation and exhalation phases, in naturally breathing anesthetized rat, without phase shift.

Averaging olfactory neural events, particularly oscillatory activity, is a challenge due to their rhythmic features. Usually, in other sensory systems, the stimulus onset of each trial is used as the time-zero reference point for data averaging. In the olfactory system, even using short stimulation, successive respiratory cycles occur during odor presentation. Thus, each respiratory cycle can be considered as a trial, and the start of inhalation period defines the time-zero reference point. Unfortunately, some fluctuations in the respiratory cycle duration arise from cycle to cycle inducing jitter in latency and making it impossible to directly average neither raw signals nor time–frequency maps as in other sensory systems (Tallon-Baudry et al., 1998). In this paper, we describe an improved method to split the respiratory cycle into its different components (inhalation, exhalation) and to transform the time component (which differed from cycle to cycle) into a phase component which is constant for all trials. This phase representation of the respiratory cycle is used as a normalized time basis to average olfactory neural events.

2. Respiration monitoring and processing

2.1. Respiratory monitoring setup

This setup is designed to record respiration in the freely breathing anesthetized rat. Since our aim is to get an accurate

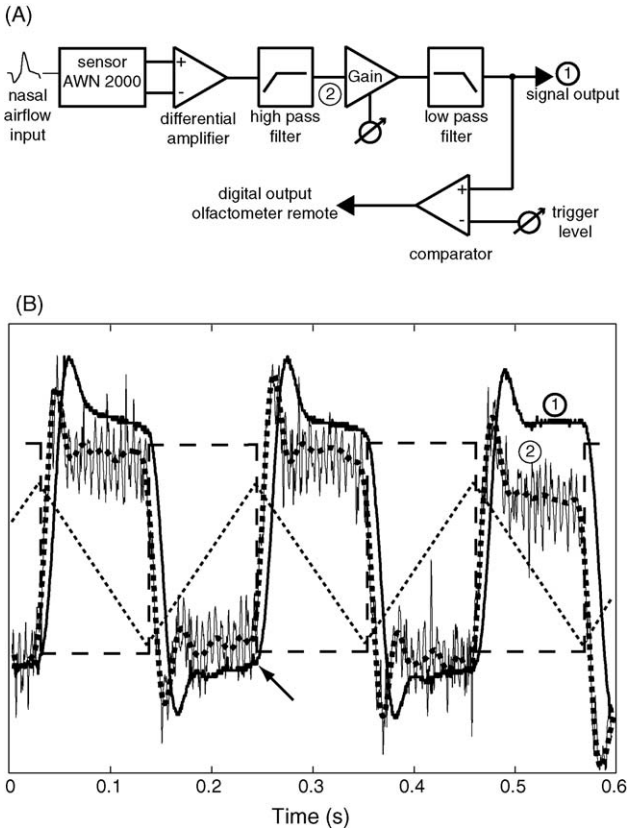

Fig. 1. (A) Schematic diagram of the electronic setup. The detected respiratory signal is high pass filtered (0.1 Hz) to avoid signal offset, amplified (with adjustable gain) and low pass filtered (30 Hz). A digital output is connected to the olfactometer; odor onset is triggered at the end of the rising phase of the expiratory period. (B) Respiratory monitoring setup test. Dotted thin line: 4.7 Hz loudspeaker electrical triangle input. Dashed line: loudspeaker theoretical pressure square output. Solid thin line: signal output before low pass filter (2). Dotted thick line: offline low pass (50 Hz) digital filtering of non-filtered signal ("filtfilt.m" Matlab function and filter designed with FIR function). Solid thick line: monitoring setup signal output (1). Different signals were normalized to be directly compared. If the slope of the signal is slightly modified by low pass filtering, the reaction time to airflow direction change remains negligible (arrow).

image of the different respiratory cycle periods and particularly their transition epochs, this recording setup is designed to quickly react to nasal airflow direction change. A direct measurement of nasal airflow is a challenge in small animal due to technical considerations: airtightness around the nostril should be total; dead volume should be as small as possible to avoid asphyxia. Moreover, such a monitoring setup makes it difficult to deliver odor stimulation and eliminate residual odor. Therefore, we chose to measure micropressure changes induced by nasal airflow in front of the nostril. The respiratory monitoring setup is described in Fig. 1A. A 10 cm long pipe samples the pressure at the edge of the nostril. The nasal airflow induces a micropressure at the pipe inlet which leads to an airflow in the pipe, measured by a thermodilution airflow sensor (bidirectional micro bridge mass airflow sensor, AWM 2000 family, Micro Switch Honeywell). This sensor is based on a constant temperature operating Wheatstone bridge, allowing fast response time (<1 ms) and thus no significant phase shift in our experimental conditions (Fig. 1B). The

bidirectionality of this sensor is essential for recording the different components of the respiratory cycle (inhalation/exhalation, respectively, underpressure/superpressure). The signal is then amplified, filtered (Fig. 1A) and digitalized with a Wavebook 512A device (IOtech) along with the electrophysiological signals (sampling rate 10 kHz). The respiratory signal is used to trigger the olfactometer (Fig. 1A); odor onset is triggered near the maximum of the expiration phase to ensure that the nominal odor concentration is reached before the beginning of the following inspiratory period.

The efficiency of our sensor was tested by using a loudspeaker emulated as a plunger (i.e. used below its resonance frequency). When passed through the loudspeaker (SP-60/8, Monacor International), a triangle electrical input is converted into a square airflow output since the loudspeaker membrane shifting is directly proportional to the applied voltage. Result of testing is shown in Fig. 1B. Since respiratory frequency extends from 1 to 4 Hz in the anesthetized rat, we chose to test our setup at a higher frequency (about 5 Hz) which is the most unfavorable conditions. Even at this higher frequency, the recording setup reacts to airflow direction change with negligible time delay regarding the total duration of the respiratory cycle (Fig. 1B). Other time points, such as peaks of inspiration or expiration, can be slightly time-shifted (a few milliseconds) by analog low pass filtering. Nevertheless, this time shift is limited regarding the total duration of the respiratory cycle. If higher precision is needed, this time shift can be avoided by recording high pass filtered signal and using offline digital filtering (Fig. 1B).

2.2. Respiratory phase computation

Using this monitoring setup, natural breathing signal appears as a periodic phenomenon showing alternating negative deflection (inspiration) and positive deflection (expiration) (Fig. 2A). The expiratory phase can be divided into a dynamic phase and a plateau extending this dynamic period (Fig. 2A).

Previous data revealed the physiological importance of the transition point between inhalation and exhalation (I/E transition) (Buonviso et al., 1992, 2003; Chaput et al., 1992; Litaudon et al., 2003; Wilson, 1998). Methods usually used to extract a phase from this signal (Hilbert transform) did not detect accurately this point because of the asymmetrical nature of the respiratory signal. With the respiratory monitoring setup described in this paper, the I/E transition is a clear zero-crossing of the rising phase of the signal (Fig. 2B) which is easily defined. Peaks of inhalation and exhalation phases are easily detected as the signal maxima and minima between two consecutive I/E points. Inhalation onset (E/I point) is the other reference point as it marks the incoming of odor stimulation. This point is the last point of the plateau extending the dynamic phase of the exhalation, and is much more difficult to automatically detect. After smoothing with a FFT-based low pass filter (30 Hz), this detection is automatically performed by detecting the point which fulfills the two following criteria: (1) its amplitude is below a first threshold (usually 10% of the maximum negative deflection) and (2) its first derivative is negative and higher than a second threshold

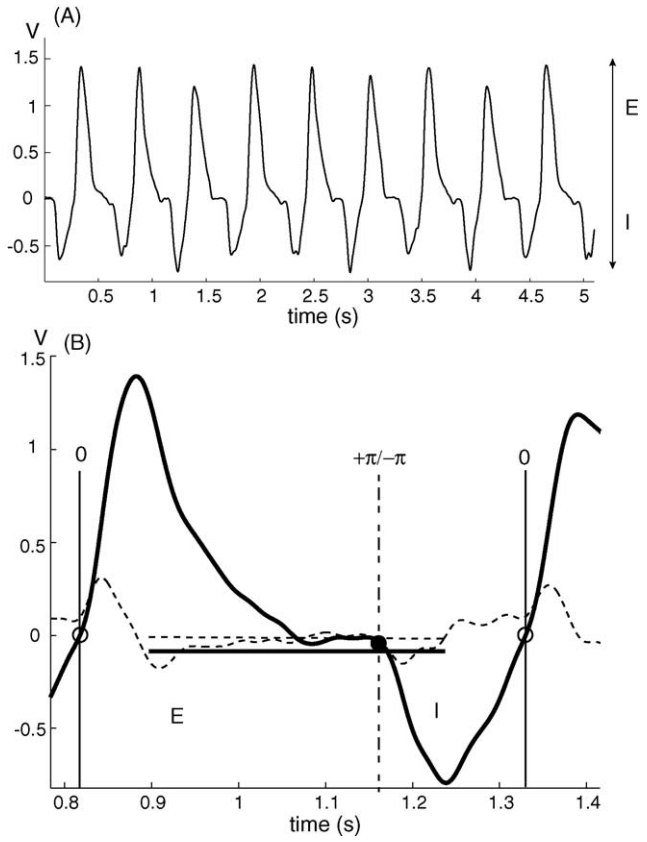

Fig. 2. (A) Respiratory signal. Positive and negative deflections correspond to expiration (E) and inspiration (I), respectively. (B) Respiratory phase detection. Solid thick line: respiratory trace; dotted line: first derivative of respiratory trace. The I/E transition point (open circle) corresponds to the zero-crossing of the respiratory trace rising phase. The E/I transition point (filled circle) is the last point of the plateau extending the dynamic phase of the exhalation which meets two criteria: its amplitude is above an amplitude threshold (horizontal solid line: 10% of the maximum negative deflection of the respiratory trace) and its derivative is negative and lower than a derivative threshold (horizontal dotted line: 10% of the maximum derivative signal).

(10% of the maximum value of the first derivative) (Fig. 2B). From now on, the time component of the respiratory signal is converted into a phase component where 0 represents the I/E transition point and π the E/I point. The phases of the inspiration and expiration are taken linearly between $[-\pi, 0]$ and $[0, \pi]$, respectively (Fig. 2B).

From a total of 1500 recordings, less than 1% failed to be processed with the phase computation method described above. Using a PC-based computer (Pentium 4), analysis of 15 s recording (sampling rate: 10 kHz, respiratory frequency: 2 Hz) takes less than 1 s.

3. Application to olfactory neural events averaging

3.1. Data acquisition

Experimental procedures have been previously explained in details (Buonviso et al., 2003; Litaudon et al., 2003). Briefly, preparation and recordings are carried out in naturally breathing, urethan (1.5 g/kg) anesthetized, Wistar rats. Anesthesia is

maintained by supplemental doses when necessary. All surgical procedures are conducted in strict accordance with the European Communities Council guidelines. Extracellular activity is recorded in the OB and in the piriform cortex using either a glass micropipette or a multichannel silicon probe (NeuroNexus Technology). Odors are presented for 5 s with a flow dilution olfactometer.

Respiratory signal is recorded as explained above. Extracellular activity is recorded as a broadband signal (0.1–5 kHz) and signals are amplified, sampled (10 kHz) and acquired on a computer using the IOTech acquisition system (Wavebook 512A).

3.2. Signal processing

Both respiratory and electrophysiological signals are processed using custom software written in Matlab (The Math Works Inc.) and C language. Unit activity is extracted by bandpassing the raw broadband signal from 300 to 3000 Hz and spikes are sorted offline, if necessary, using an algorithm implemented in Matlab (The Math Works Inc.).

Since our aim is to identify and characterize LFP oscillatory activities in time and frequency, we choose a method that preserves both types of information, i.e. a time–frequency representation based on a wavelet transform of the signal (Fig. 3A, left). The LFP signal is first down-sampled (200 Hz) and then convoluted by complex Morlet's wavelets $w(t,\ f_0)$ (Kronland-Martinet et al., 1987) which have a Gaussian shape both in the time domain and in the frequency domain around its central frequency f_0:

$$\text{with}\ \ w(t,\ f_0) = A \exp\left(\frac{t^2}{2}\right) \exp(i2\pi f_0 t)$$

The wavelet family we use is defined by $\omega_0 = 2\pi f_0 = 5$, with f_0 ranging from 0 to 100 Hz in 1 Hz step. The time resolution of the wavelet method increases with frequency, whereas the frequency resolution decreases. The time-varying energy $E(t,\ f_0)$ of the signal in a frequency band around f_0 is defined as the square of the convolution product of the wavelet $w(t,\ f_0)$ with the signal $s(t)$:

$$E(t,\ f_0) = [w(t,\ f_0) * s(t)]^2$$

3.3. Data averaging

3.3.1. Local field potential oscillatory activity averaging

As previously explained, respiratory cycle duration slightly varies either during a trial or between different recording sessions. Therefore, rhythmic induced activity appears with jitter in latency from cycle to cycle making it impossible to directly average time–frequency maps. However, this could be achieved by using a phase representation of the respiratory cycle which provides a normalized time basis for data averaging. The time–frequency map (Fig. 3A, left) is transformed into respiratory phase-frequency maps (Fig. 3A, right) as follows: based on respiratory phase previously extracted, the time–frequency map computed with Morlet wavelet is first segmented into successive respiratory cycles with alternating inspiration and expiration windows (Fig. 3A, left). Each window is resampled (line by line) with a Fast Fourier Transform method in order to obtain a width identical for each window. This width in pixel depends on the precision required. The phases of the inspiration and expiration windows are taken linearly between $[-\pi,\ 0]$ and $[0,\ \pi]$, respectively, as previously explained. Thus, the time–frequency map is rescaled as a respiratory phase-frequency map with alternating inhalation and exhalation phases (Fig. 3A, right). As opposed to time scale, phase scale is reproducible from trial to trial and the phase representation of the respiratory cycle defines the "time basis" which will be used for data averaging. The use of such phase-frequency maps is particularly interesting for averaging LFP oscillatory activities which have been shown to be modulated by breathing (Buonviso et al., 2003). These oscillatory activities are not phase-locked from trial to trial precluding the use of direct raw signal averaging. Fig. 3B (left) shows the scalogram resulting from averaging time–frequency maps (Tallon-Baudry et al., 1998) using the start of the first inhalation period following odor onset as the time-zero reference point. As can be seen, the spots of high activity in the gamma range become progressively blurred and disappear across successive respiratory cycles due to fluctuations in respiratory cycle duration. Conversely, those spots remain distinct across cycles when phase-frequency maps are used (Fig. 3B, right). From phase-frequency maps, we can also compute the mean representation of activity related to respiratory cycle (Fig. 3C, left). Such representation allows accurate calculation of the average phase of oscillatory activity in the different frequency bands which can be used for following statistical analysis. In Fig. 3C, we compare our respiratory cycle segmentation based on two reference point (I/E and E/I, left) with previous methods using only one reference point (I/E transition, right). If the zero phase is accurately defined as the I/E transition point using both methods, the $-\pi/\pi$ phase differs according to the method used. With the method described in this paper, $-\pi/\pi$ is clearly defined as the E/I transition. With the previous method, $-\pi/\pi$ corresponds to the intermediate value between two consecutive I/E points, and cannot be directly related to a respiratory epoch. Consequently, the phase of gamma activity, which is phase-locked with I/E transition, is accurately defined with both methods (Fig. 3C). By contrast, the phase of beta activity which is phase-locked with other respiratory epochs, is more loosely defined when using one reference point segmentation.

3.3.2. Unitary activity averaging

The main application of the respiratory signal processing presented in this paper is to compute oscillatory neural events averaging. But it can also be used to compute a respiratory cycle-triggered raster plot which is a commonly used representation of both bulbar and cortical cell response patterns (Buonviso et al., 1992, 2003; Chaput et al., 1992; Litaudon et al., 2003; Wilson, 1998). First, each spike is time-stamped from the raw signal. Based on the previously extracted respiratory phase, this time position is converted into a phase position relative to the res-

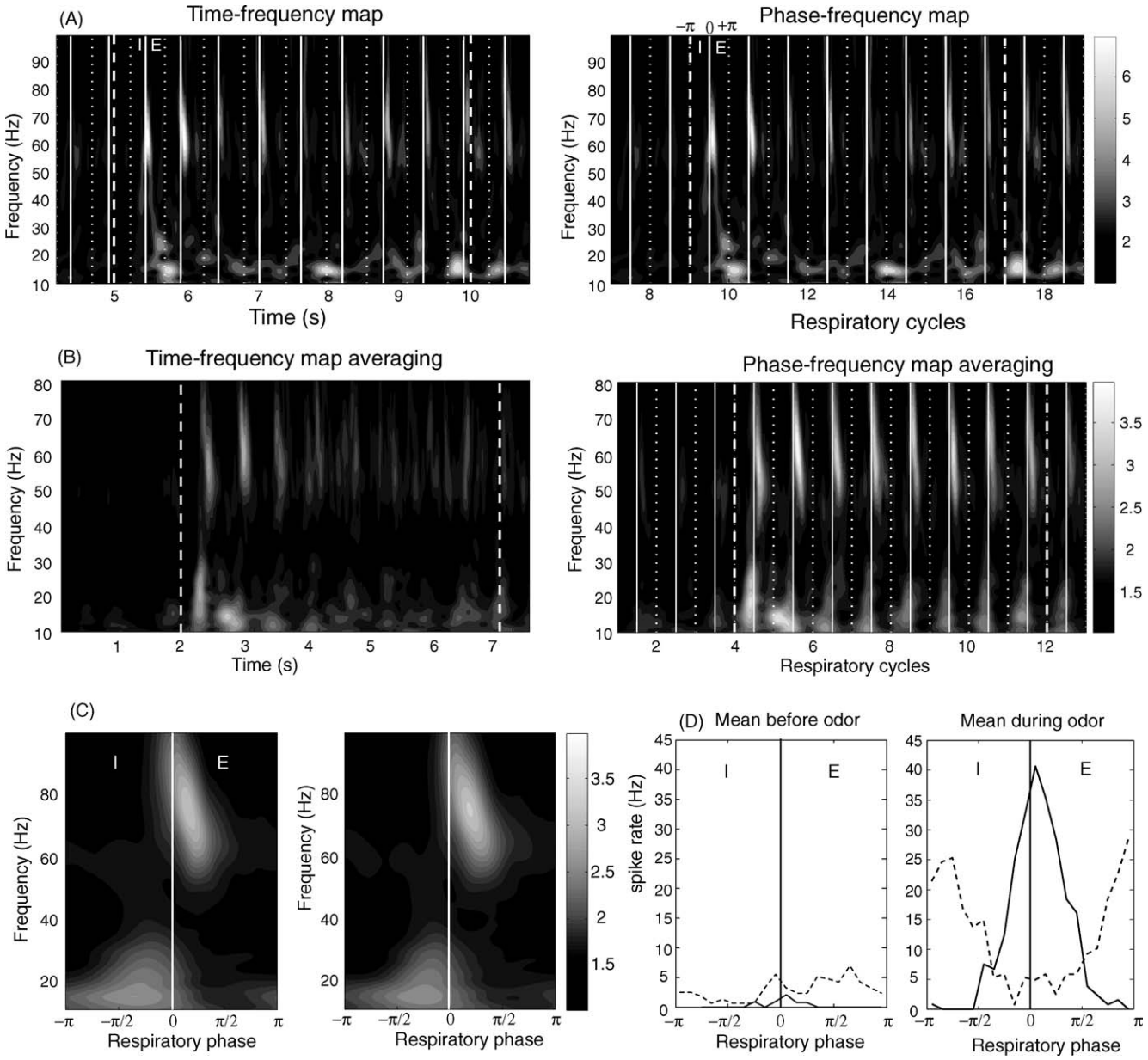

Fig. 3. Oscillatory signal processing and data averaging. (A) time–frequency map (left) and phase-frequency map (right) of the LFP signal recorded in the main OB in response to amyl acetate stimulation (5 s, concentration: 1.8 10^{-1} of the saturated vapor pressure). White solid line and dotted line indicated I/E and E/I transition point, respectively. Dashed line indicates beginning and end of odor stimulation. Gray scale: energy representation is normalized relative to prestimulus total energy. (B) Mean oscillatory activity evoked by amyl acetate ($n = 19$ animals, 1 odor presentation per animal) computed from time–frequency maps (left) or phase-frequency maps (right). (C) Averaged respiratory cycle frequency maps during odor stimulation computed from data used in (B). Computation with respiratory cycle segmentation using both I/E and E/I reference points (left) and I/E reference point only (right). Notice the gamma activity (40–80 Hz) located around the I/E transition point and the beta activity (15–30 Hz) limited to inspiration. (D) Example of two types of averaged synchronized cell responses recorded in the anterior piriform cortex (coordinates relative to bregma: AP = 2.5 mm; ML = 3.5 mm) before (left) and during (right) odor presentation. Averaged I/E synchronized response ($n = 6$ cells, solid line) and averaged E/I synchronized response ($n = 8$ cells, dotted line). Instantaneous frequency is computed along each respiratory cycle (short sliding window, 50 ms) and average spike rate is calculated relative to the respiratory cycle phase.

piratory cycle which is used to compute histograms of phase distribution along the respiratory cycle. As previously reported (Buonviso et al., 1992, 2003; Chaput et al., 1992; Litaudon et al., 2003), this phase representation can be used to classify response patterns as a function of the respiratory activity. Moreover, it allows to compute the average activity of a given cell response category collected from different trials (Fig. 3D).

4. Conclusion

The present paper describes a rapid and accurate automatic method to analyze respiratory phases. Such method allows to process a large amount of data as compared to manual analysis that are not only time-consuming but can also result in some bias due to human subjectivity. Such an automatic method would not

be possible without a well-suited respiratory recording setup which preserves the temporal course of the respiratory cycle. In this paper, we describe a low cost respiratory monitoring setup which presents several advantages. The detector is located close to the olfactory input compared to piezoelectric devices which gives an indirect image of the nasal airflow through chest-wall movements. Detector positioning is easy and non-invasive compared to thermocouple (Macrides et al., 1982; Uchida and Mainen, 2003). Lastly, this setup is very sensitive and can be used with smaller animal, such as rat pups or mice. This setup is developed to record respiratory activity in anesthetized animals and cannot be used in freely moving rats as implanted thermocouple (Macrides et al., 1982; Uchida and Mainen, 2003).

In previous papers (Buonviso et al., 2003; Litaudon et al., 2003), respiratory phase was taken linearly between two consecutive I/E transition points. Although if the phase of I/E phase-locked activities remained accurately defined (Fig. 3C, right), activities which are phase-locked with other respiratory epochs were more loosely defined since the actual start of the inspiration phase could not be evaluated. The accurate estimation of the E/I transition point is of great importance as it defines the input of sensory information and can be used as the reference point for data averaging. If the analysis presented in the present paper focused on phase relationship between respiratory activity and olfactory neural events, reference points can also be used to evaluate their temporal relationships (Macrides et al., 1982). With the method described in this paper, the precision of analysis can be set by the experimenter. In the example shown in this paper, we used two reference points (I/E and E/I transition points) but maxima of inspiration and expiration could also be considered. A very precise determination of different reference points in the respiratory cycle allows accurate analysis of the temporal distribution of olfactory neural events. Such analysis is of great importance regarding the high speed of odor discrimination that can be achieved in only one sniff (Abraham et al., 2004; Uchida and Mainen, 2003).

The use of the respiratory cycle as a "time basis" provides tools to analyze the role of oscillatory activity in olfactory information processing and permits to collect results in a standardized data format that allows comparisons and averaging across different animals.

References

Abraham NM, Spors H, Carleton A, Margrie TW, Kuner T, Schaefer AT. Maintaining accuracy at the expense of speed: stimulus similarity defines odor discrimination time in mice. Neuron 2004;44:865–76.

Adrian ED. The electrical activity of the mammalian olfactory bulb. Electroencephalogr Clin Neurophysiol 1950;2:377–88.

Boudreau JC, Freeman WJ. Spectral analysis of electrical activity in the prepyriform cortex of the cat. Exp Neurol 1963;8:423–39.

Buonviso N, Chaput MA, Berthommier F. Temporal pattern analyses in pairs of neighboring mitral cells. J Neurophysiol 1992;68:417–24.

Buonviso N, Amat C, Litaudon P, Roux S, Royet JP, Farget V, et al. Rhythm sequence through the olfactory bulb layers during the time window of a respiratory cycle. Eur J Neurosci 2003;17:1811–9.

Chaput MA, Holley A. Single unit responses of olfactory bulb neurones to odour presentation in awake rabbits. J Physiol (Paris) 1980;76:551–8.

Chaput MA. Respiratory-phase-related coding of olfactory information in the olfactory bulb of awake freely-breathing rabbits. Physiol Behav 1986;36:319–24.

Chaput MA, Buonviso N, Berthommier F. Temporal patterns in spontaneous and odour-evoked mitral cell discharges recorded in anaesthetized freely breathing animals. Eur J Neurosci 1992;4:813–22.

Fontanini A, Spano P, Bower JM. Ketamine-xylazine-induced slow (<1.5Hz) oscillations in the rat piriform (olfactory) cortex are functionally correlated with respiration. J Neurosci 2003;23:7993–8001.

Freeman WJ. Mass action in the nervous system. New York: Academic Press; 1975.

Freeman WJ, Schneider W. Changes in spatial patterns of rabbit olfactory EEG with conditioning to odors. Psychophysiology 1982;19:44–56.

Freeman WJ. The physiological basis of mental images. Biol Psychiatry 1983;18:1107–24.

Johnson BN, Mainland JD, Sobel N. Rapid olfactory processing implicates subcortical control of an olfactomotor system. J Neurophysiol 2003;90:1084–94.

Kronland-Martinet R, Morlet J, Grossmann A. Analysis of sound patterns through wavelet transforms. Int J Patt Recognit Artif Intell 1987;1:273–302.

Litaudon P, Amat C, Bertrand B, Vigouroux M, Buonviso N. Piriform cortex functional heterogeneity revealed by cellular responses to odours. Eur J Neurosci 2003;17:2457–61.

Macrides F, Chorover SL. Olfactory bulb units: activity correlated with inhalation cycles and odor quality. Science 1972;175:84–7.

Macrides F, Eichenbaum HB, Forbes WB. Temporal relationship between sniffing and the limbic rhythm during odor discrimination reversal learning. J Neurosci 1982;2:1705–17.

Mair RG. Response properties of rat olfactory bulb neurones. J Physiol 1982;326:341–59.

Margrie TW, Schaefer AT. Theta oscillation coupled spike latencies yield computational vigour in a mammalian sensory system. J Physiol 2003;546:363–74.

Onoda N, Mori K. Depth distribution of temporal firing patterns in olfactory bulb related to air-intake cycles. J Neurophysiol 1980;44:29–39.

Pager J. Respiration and olfactory bulb unit activity in the unrestrained rat: statements and reappraisals. Behav Brain Res 1985;16:81–94.

Spors H, Grinvald A. Spatio-temporal dynamics of odor representations in the mammalian olfactory bulb. Neuron 2002;34:301–15.

Tallon-Baudry C, Bertrand O, Peronnet F, Pernier J. Induced γ-band activity during the delay of a visual short-term memory task in humans. J Neurosci 1998;18:4244–54.

Uchida N, Mainen ZF. Speed and accuracy of olfactory discrimination in the rat. Nat Neurosci 2003;6:1224–9.

Walsh RR. Single cell spike activity in the olfactory bulb. Am J Physiol 1956;186:255–7.

Wilson DA. Habituation of odor responses in the rat anterior piriform cortex. J Neurophysiol 1998;79:1425–40.